

Research on Dead-Beat Control Method for Grid-Connected Inverter Stability Prediction

Li Jun¹

¹*School of Electrical and Electronic Engineering, HUAZHONG University of science and technology, wuhan ,430074, China
1404322@qq.com*

Abstract

In the photovoltaic micro-grid control system, delay and filter inductance change can influence system response speed, stability and grid-connected current distortion rate. Therefore, a power feed-forward dead-beat grid-connection control method for robustness prediction is proposed in this paper. The power feed-forward control is introduced therein to accelerate the system response speed, and the dead-beat control method for robustness prediction is proposed for the grid-connected current control in order to strengthen system robustness and reduce the grid-connected current distortion caused by control delay and inductance deviation. Specifically, Z-domain dead-beat control model with delay link is analyzed in this paper in order to discuss the influence of delay and inductance on system stability and accordingly provide the dead-beat control design method for robustness prediction as well as analyze the stability thereof according to the transfer function in Z-domain, thus to determine the control parameter scope. Moreover, the simulation experiment results have verified the effectiveness of the proposed control method.

Keywords: *Photovoltaic grid-connection; Dead-beat control; Inverter; Power feed-forward; Robustness prediction*

1. Introduction

As an emerging advanced technology developed on the basis of new energy distributed generation, the micro-grid plays a role in mutual support with large power grid and is an effective method for improving the distributed generation energy supply efficiency [1-2]. In future, more and more distributed micro-grids involving new energy power generation will appear in small and medium smart distribution networks. Currently, the weakness of the large power grids becomes more and more obvious. Therefore, it is necessary to integrate the geographically-adjacent key loads into micro-grids and design suitable circuit topology and control method in order to not only reduce the necessary costs incurred for improving overall reliability and power quality, but also reduce the economic losses caused by power outage [3-5].

In the photovoltaic grid-connected inverter control system, delay and filter inductance change of the digital system can influence system response speed, stability and grid-connected current distortion rate. Therefore, a power feed-forward dead-beat grid-connection control method for robustness prediction is proposed in this paper. The power feed-forward control is introduced therein to accelerate the system response speed, and the dead-beat control method for robustness prediction is proposed for the grid-connected current control in order to strengthen system robustness and reduce the grid-connected current distortion caused by control delay and inductance deviation. Specifically, Z-domain dead-beat control model with delay link is analyzed in this paper in order to discuss the influence of delay and inductance on system stability and accordingly provide the dead-beat control design method for robustness prediction as well as analyze the

stability thereof according to the transfer function in Z-domain, thus to determine the control parameter scope. Moreover, the simulation experiment results have verified the effectiveness of the proposed control method.

2. Photovoltaic Grid-Connected Inverter Dead-Beat Control Principle

2.1. VSI System Modeling

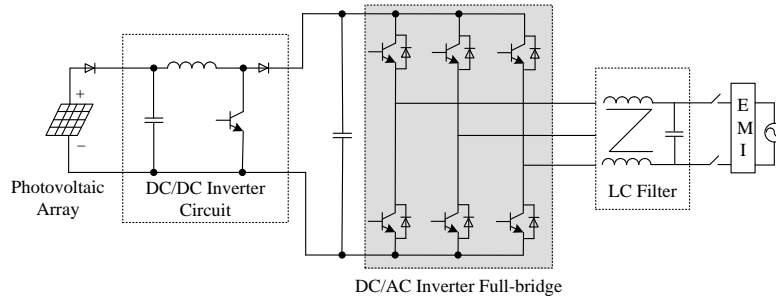


Figure 1. Three-Phase Photovoltaic Grid-Connected Inverter System Structure

Figure 1, shows the structural block diagram of the three-phase photovoltaic grid-connected inverter system, mainly including two parts ---- front DC/DC inverter and three-phase DC/AC grid-connected inverter. Under the assumption that the three-phase network voltage is balanced and the switching loss and the voltage drop of the power switch are ignored, the following mathematical model for the photovoltaic grid-connected VSI system is established in two-phase static $\alpha\beta$ coordinate system according to Kirchhoff's law:

$$\mathbf{u}_{g\alpha\beta} = \mathbf{v}_{g\alpha\beta} + L_g \frac{d\mathbf{i}_{g\alpha\beta}}{dt} + R_g \mathbf{i}_{g\alpha\beta} \quad (1)$$

Where $\mathbf{u}_{g\alpha\beta}$ is the component of the network voltage under $\alpha\beta$ coordinate system; $\mathbf{v}_{g\alpha\beta}$ is the component of the grid-connected VSI terminal voltage under $\alpha\beta$ coordinate system; $\mathbf{i}_{g\alpha\beta}$ is the component of the network current under $\alpha\beta$ coordinate system; L_g is the filter reactor at the network side, and R_g is the equivalent resistance.

According to the instantaneous reactive power theory, the instantaneous active power and the instantaneous reactive power of the three-phase symmetrical system can be described as follows:

$$\begin{cases} P_g = -1.5(u_{g\alpha}i_{g\alpha} + u_{g\beta}i_{g\beta}) \\ Q_g = -1.5(u_{g\beta}i_{g\alpha} - u_{g\alpha}i_{g\beta}) \end{cases} \quad (2)$$

In order to find the change rate of the instantaneous active power and the instantaneous reactive power, Formula (2) is differentially processed as follows:

$$\begin{cases} \frac{dP}{dt} = -1.5 \left(e_\alpha \frac{di_\alpha}{dt} + i_\alpha \frac{de_\alpha}{dt} + e_\beta \frac{di_\beta}{dt} + i_\beta \frac{de_\beta}{dt} \right) \\ \frac{dQ}{dt} = -1.5 \left(e_\beta \frac{di_\alpha}{dt} + i_\alpha \frac{de_\beta}{dt} - e_\alpha \frac{di_\beta}{dt} - i_\beta \frac{de_\alpha}{dt} \right) \end{cases} \quad (3)$$

Where the change rate of the network voltage under ideal conditions is as follows:

$$\begin{cases} \frac{de_\alpha}{dt} = \omega|e|\sin(\omega t) = -\omega e_\beta \\ \frac{de_\beta}{dt} = \omega|e|\cos(\omega t) = \omega e_\alpha \end{cases} \quad (4)$$

Hereby, Formulae (1) and (4) are put into Formula (3) to obtain the instantaneous power change rate of the grid-connected inverter system as follows:

$$\begin{cases} \frac{dP}{dt} = -\frac{3}{2L} \left[|e|^2 - (e_\alpha v_\alpha + e_\beta v_\beta) \right] - \frac{R}{L} P - \omega Q \\ \frac{dQ}{dt} = -\frac{3}{2L} \left[-(e_\beta v_\alpha - e_\alpha v_\beta) \right] - \frac{R}{L} Q + \omega P \end{cases} \quad (5)$$

2.2. Dead-Beat Control Principle

VSI inverter as shown in Figure 1 can provide eight effective voltage vectors including six nonzero voltage vectors $\mathbf{v}1 \sim \mathbf{v}6$ and two zero voltage vectors $\mathbf{v}0$ and $\mathbf{v}7$. In each control period, only a single voltage vector acts on the grid-connected inverter, and this voltage vector is numbered as i , and the change rates of the corresponding active power and the reactive power are respectively as follows:

$$\begin{cases} s_i^p = \frac{dP}{dt} | \mathbf{v} = \mathbf{v}_i \\ s_i^q = \frac{dQ}{dt} | \mathbf{v} = \mathbf{v}_i \end{cases} \quad (6)$$

$Td0$ delay exists between the system sampling point and PWM action moment, but the influence of such delay is too small to be ignored relatively to PWM action effect. At the end of the control period, P and Q tracking error loci are as follows:

$$\begin{cases} E_p = P^* - P^{k+1} = P^* - P^k - S_a^p T_a - S_b^p T_b - S_c^p T_c \\ E_q = Q^* - Q^{k+1} = Q^* - Q^k - S_a^q T_a - S_b^q T_b - S_c^q T_c \end{cases} \quad (7)$$

In order to maximally restrain the power pulsation phenomenon and realize dead-beat tracking control effect, the least square method is adopted to construct the following power tracking error value function:

$$g = E_p^2 + E_q^2 \quad (8)$$

The derivatives of Formula (9) to T_a and T_b are solved as follows:

$$\begin{cases} \frac{\partial g}{\partial T_a} = 0 \\ \frac{\partial g}{\partial T_b} = 0 \end{cases} \quad (9)$$

Formulae (8) ~ (10) are combined to obtain the action time of three voltage vectors.

3. Influence of Delay on Dead-Beat Control Stability

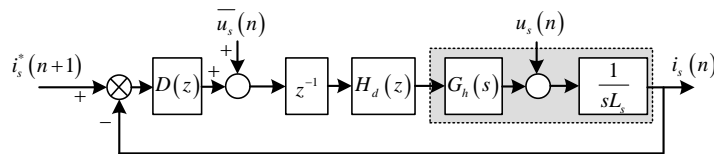


Figure 2. Dual-Level VSI Voltage Space Vector Distribution Diagram

In consideration of the control delay problem existing in practical digital processing system, the equivalent model for Z-domain dead-beat control involving VSI system delay is given in Figure 2. Therein, the transfer function of the zero-order holder (ZOH) is as follows:

$$G_h(s) = (1 - e^{-Ts}) / s \quad (10)$$

Then, Z-domain transfer function of zero-order holder and the inductor is as follows:

$$G_d(z) = (1 - z^{-1}) Z \left[\frac{1}{s} \frac{1}{sL_s} \right] = \frac{T_s}{L_s} \frac{1}{z-1} \quad (11)$$

Since the transfer function of delay link z^{-1} can be represented as $e^{-T_d s}$, thus the following formula can be obtained through Taylor series expansion:

$$e^{-T_d s} = \frac{1}{1 + T_d s + T_d^2 s^2 / 2 + L} \approx \frac{1}{1 + T_d s} \quad (12)$$

L_s is assumed as the predicted value of the grid-connected inductance and has certain deviation from actual inductance Z , wherein the deviation degree thereof is measured through the inductance coefficient, namely: if $kL = L_s/L_s$ is true, then $D(z) = kL L_s / T_s$ is true. If the proportionality coefficient of PWM delay is assumed as $kT = T_d / T_s$, then the transfer function of delay link T_d can be represented as follows:

$$H_d(z) = [(1 - k_T)z + k_T] / z \quad (13)$$

In conclusion, the closed-loop transfer function of the system with delay link td is as follows:

$$G(z) = \frac{D(z)z^{-1}H_d(z)G_d(z)}{1 + D(z)z^{-1}H_d(z)G_d(z)} \quad (14)$$

At this moment, the characteristic equation of the closed-loop system is as follows:

$$z^3 - z^2 + k_L(1 - k_T)z + k_L k_T = 0 \quad (15)$$

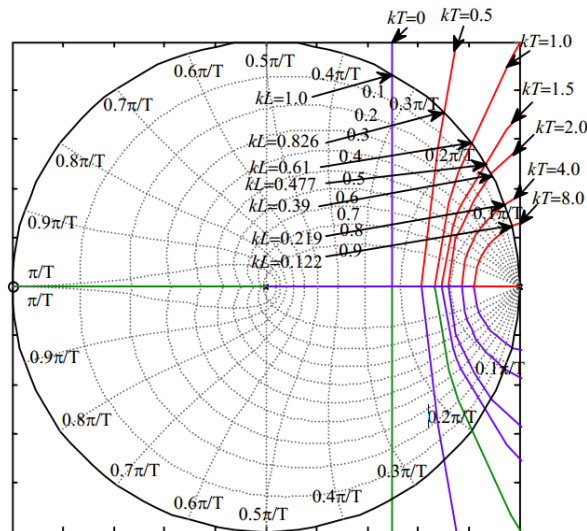


Figure 3. Diagram for Different Root Loci When Changing kT From 0 to 8

When kT is changed from 0 to 8, different root loci are as shown in Figure 3. In the stability range, compared with the one-lag control, the upper limit of kL is gradually reduced along with the increase of delay coefficient kT . In other words, the predicted value of the inductance is required to be smaller and smaller, but kT reduction will reduce system control accuracy and influence the stability of the grid-connected inverter system.

4. Dead-Beat Control Method for Robustness Prediction

In allusion to the unmatched control delay and model inductance in the grid-connection process, a dead-beat control method for robustness prediction is proposed in this paper. Specifically, the grid-connected current and the network voltage are predicted in order to estimate the grid-connected current and the network voltage of the next sampling period, thus to maintain the grid-connection synchronization through the advanced control for improving the robustness of the grid-connected inverter. According to the dead-beat control method, Formula (1) can be changed as follows:

$$u_{inv}(n) = \hat{u}_{s_av}(n+1) + \frac{k_L k_s}{T_s} \left[\hat{i}_s^*(n+1) - \hat{i}_s(n+1) \right] \quad (16)$$

Where $i_s(n+1)$ is the predicted value of the grid-connected current at sampling time $(n+1)$; $u_{s_av}(n+1)$ is the predicted average value of the network voltages in the sampling period; $u_s(n)$ is the sampling value of the network voltage at time n ; $u_s(n-1)$ is the sampling value of the network voltage at time $n-1$.

Linear interpolation is implemented for $u_s(n)$ and $u_s(n-1)$ to obtain the predicted average value $u_{s_av}(n+1)$ of the network voltages in sampling period $(n+1)$ as follows:

$$\begin{cases} \hat{u}_{s_av}(n) = \left[\hat{u}_s(n+1) + u_s(n) \right] / 2 \\ \hat{u}_s(n+1) = 2u_s(n) - u_s(n-1) \end{cases} \quad (17)$$

Since the grid-connected current can cause the change of the filter inductance output by the inverter, thus the linear interpolation is no longer suitable for the grid-connected current prediction. Therefore, a nonlinear interpolation method is proposed and applied to the grid-connected current prediction. Specifically, the sampling value of the grid-connected current at sampling time n and the weight factor m ($0 < m < 1$) are adopted to obtain the predicted value of the grid-connected current at sampling time $(k+1)$ as follows:

$$\hat{i}_s(n+1) = m \hat{i}_s(n) + (1-m) \cdot i_s(n) + \frac{T_s}{k_L L_s} \left[u_{inv}(n-1) - \hat{u}_{s_av}(n) \right] \quad (18)$$

The structural block diagram of the dead-beat control link for the robustness prediction in the current inner-loop is as shown in Figure 4.

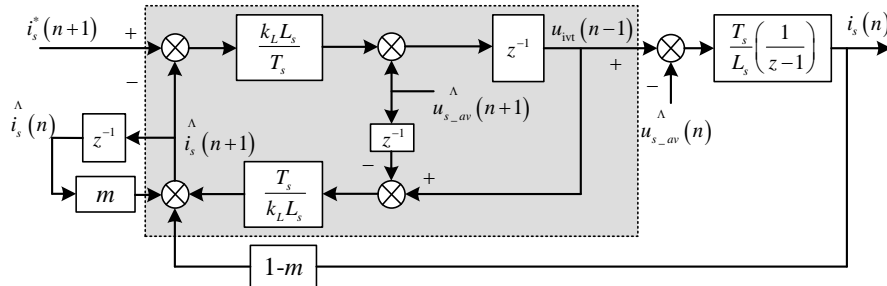


Figure 4. Structural Block Diagram of Dead-Beat Control Link for Robustness Prediction in Current Inner-Loop

The closed-loop transfer function of the current inner-loop is as follows:

$$\hat{i}_s(n+1) = m \hat{i}_s(n) + (1-m) \cdot i_s(n) + \frac{T_s}{k_L L_s} \left[u_{inv}(n-1) - \hat{u}_{s_{av}}(n) \right] \quad (19)$$

If $kL \approx 1$ is true, then the transfer function is $G(z)=z^{-2}$. For any m value, the control is delayed for two sampling periods. The closed-loop characteristic equation is as follows:

$$P(z) = z^2 - mz + (k_L - 1)(1 - m) = 0 \quad (20)$$

According to Jury stability criterion, the change range of kL is as follows:

$$0 < k_L < 1 + \frac{1}{1-m} \quad (21)$$

Obviously, compared with traditional synchronous dead-beat control, for an arbitrary value, the dead-beat control for current robustness prediction can strengthen system stability margin. Figure 5, shows the root locus of the dead-beat control system with one sampling period delay for robustness prediction, wherein W is changed from 0 to 0.99 in Z-domain.

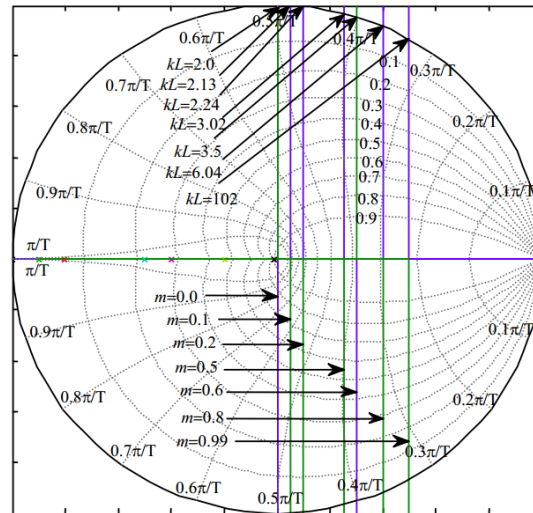


Figure 5. Root Locus Diagram of Current Robustness Prediction Control System with 1 Sampling Period Delay

According to the root loci, the upper limit is rapidly and progressively increased along with the increase of m in the stability domain. Compared with the traditional dead-beat control, the allowable range of the inductance deviation of the model is expanded, and the robustness of the grid-connected inverter system is obviously improved.

5. Experiment Result and Analysis

In order to verify the superiority of the proposed dead-beat control method for the robustness prediction of the grid-connected inverter in the aspects of system stability improvement, and the feasibility of the robust dead-beat control method is analyzed in 35kW photovoltaic grid-connected inverter experiment platform as shown in Figure 6. The global control block diagram for the robust dead-beat control method is as shown in Figure 7, According to the figure, the two links-power feed-forward dead-beat control and robust current dead-beat control, are added to respectively strengthen system response performance and reduce parameter sensitivity.

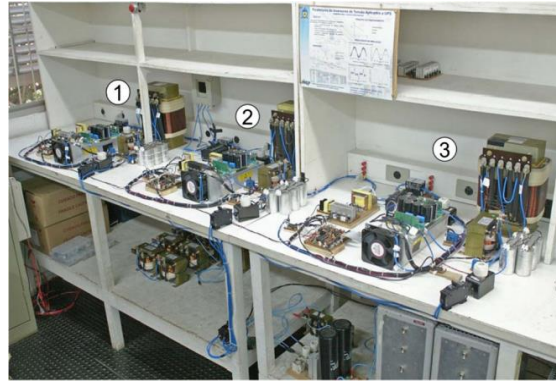


Figure 6. Experiment Platform for Photovoltaic Grid-Connection Inverter System

Figure 8, shows the steady-state experiment results of the photovoltaic grid-connected inverter system, including: a-phase grid-side current, a-phase output voltage and corresponding a-phase current spectrogram. According to the figure, the grid-side current is regularly distributed and has high sine degree, and the corresponding total distortion rate is THD=6.77% when the switching frequency is only 2kHz, and the current harmonics are mainly centralized around switching frequency 2kHz and the integral multiples thereof, thus greatly reducing the grid-connected filter design difficulty. Additionally, VSI system has fixed switching frequency, thus not only benefiting for the switching loss reduction, but also further demonstrating the validity of the three-vector selection principle of the dead-beat control based on VSI system model.

Figure 9, shows the dynamic experiment results of the photovoltaic grid-connected system, and Figure 9(a) shows the current change waveform during the process of sharply changing the given current component from 25A to 40A at 0.043s. According to the figure, under the robust dead-beat control method, the actual current only needs one sampling period (500ms) to catch up the given value, thus indicating that the proposed method has excellent dynamic performance. The variation diagram of the action time of the three vectors shown in Figure 9(b), indicates that the actual current can follow the given value in one sampling period through rapidly adjusting the action time of the three vectors during the dynamic process, thus effectively demonstrating the superiority of the power feed-forward unit in the aspects of optimizing the dynamic response performance of the system.

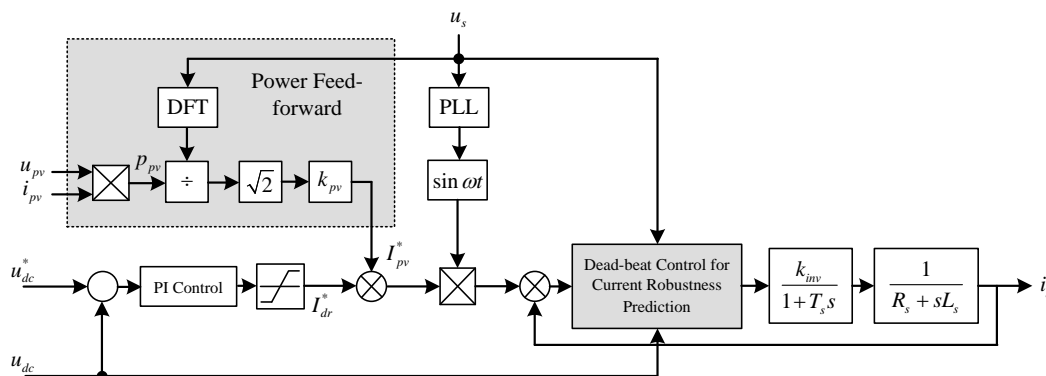


Figure 7. Global Control Block Diagram for Robust Dead-Beat Control Method

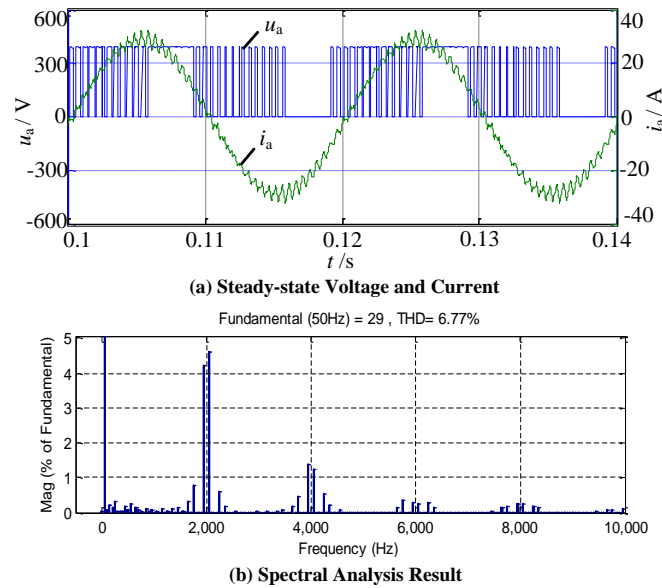


Figure 8. Steady-State Experiment Result

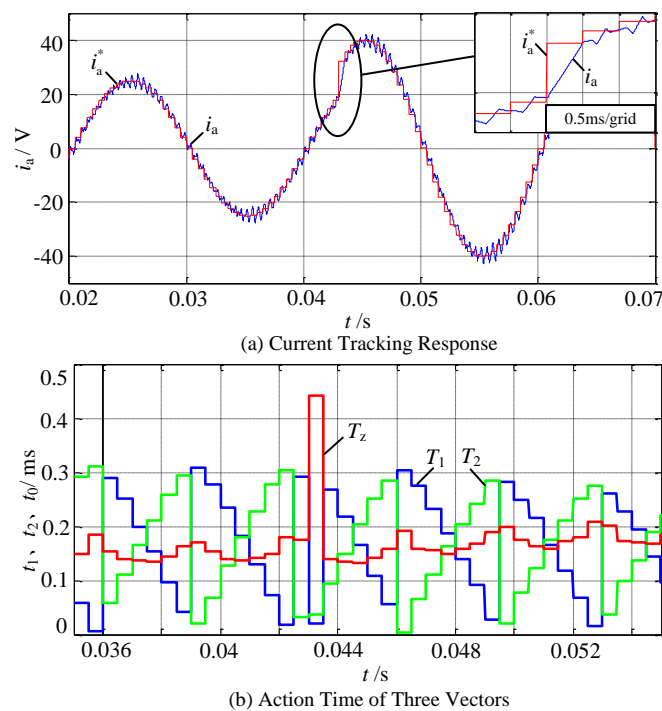
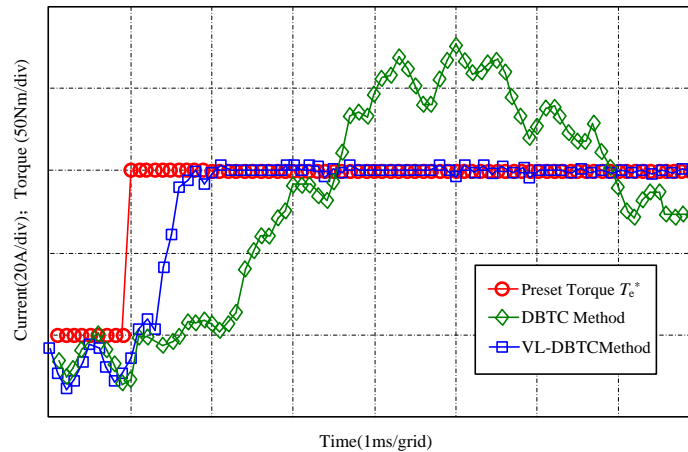


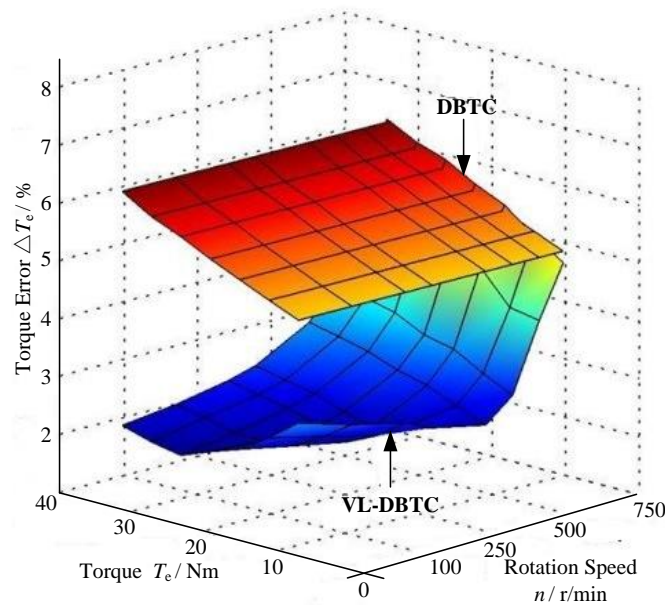
Figure 9. Dynamic Experiment Result

If the dynamic and steady-state characteristics of the robust dead-beat control and the traditional dead-beat control under parameter distortion, wherein the filter inductance parameter is set as $kL = L_s/L_s = 4$. Specifically, Figure 10(a), shows the torque response characteristics comparison experiment results of the two methods during the dynamic process, and the traditional dead-beat control has obvious vibration during the dynamic process, and when the power response time is significantly increased above 10ms, the original rapid response advantage of the dead-beat control is lost. According to the comparison, the robust dead-beat control can still maintain the excellent response characteristic and only takes at most 1ms to realize the torque response, with a linear

uniform transition process; Figure 10(b), shows the torque accuracy comparison experiment results of the two methods during the steady-state process, and due to the control delay and parameter distortion existing in practical digital processing system, VSI power tracking accuracy is significantly reduced and the power fluctuation range is up to 5%~8%. However, the robust dead-beat control method can always maintain the excellent power tracking effect and the tracking errors thereof in the whole power range are all less than those of the traditional dead-beat control method, and the experiment result further verifies the validity of the previous theoretical analysis.



(a) Current Waveform under Bus-bar Current Restriction



(b) Steady-state Accuracy Comparison Result

Figure 10. Comparison of Dynamic-State and Steady-State Characteristics of Robust Dead-Beat and Traditional Dead-Beat Under Parameter Inaccuracy

6. Conclusion

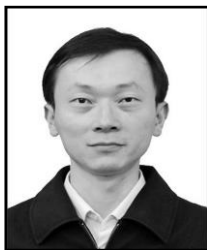
A power feed-forward dead-beat grid-connection control method for robustness prediction is researched in this paper, and the following conclusions can be obtained through relevant theoretical analysis and prototype experiment verification: according to the stability analysis of z -domain dead-beat control model with delay link, the current

control accuracy and the system stability of the traditional dead-beat control method can be easily influenced by unmatched delay and filter inductance; the dead-beat control method for current robustness prediction can effectively solve the system instability problems caused by digital system delay, parameter matching etc., thus further improving the practical application significance of the dead-beat control method.

References

- [1] T. Su, W. Wang and Z. Lv, "Rapid Delaunay triangulation for randomly distributed point cloud data using adaptive Hilbert curve", *Computers & Graphics*, vol. 54, (2016), pp. 65-74.
- [2] J. Hu, Z. Gao and W. Pan, "Multiangle Social Network Recommendation Algorithms and Similarity Network Evaluation", *Journal of Applied Mathematics*, vol. 2013, (2013).
- [3] S. Zhou, L. Mi, H. Chen and Y. Geng, "Building detection in Digital surface model", 2013 IEEE International Conference on Imaging Systems and Techniques (IST), (2012) October.
- [4] J. He, Y. Geng and K. Pahlavan, "Toward Accurate Human Tracking: Modeling Time-of-Arrival for Wireless Wearable Sensors in Multipath Environment", *IEEE Sensor Journal*, vol. 14, no. 11, (2014) November, pp. 3996-4006.
- [5] Z. Lv, A. Halawani and S. Fen, "Touch-less Interactive Augmented Reality Game on Vision Based Wearable Device", *Personal and Ubiquitous Computing*, vol. 19, no. 3, (2015), pp. 551-567.
- [6] G. Bao, L. Mi, Y. Geng, M. Zhou and K. Pahlavan, "A video-based speed estimation technique for localizing the wireless capsule endoscope inside gastrointestinal tract", 2014 36th Annual International Conference of the IEEE Engineering in Medicine and Biology Society (EMBC), (2014) August.
- [7] D. Zeng and Y. Geng, "Content distribution mechanism in mobile P2P network", *Journal of Networks*, vol. 9, no. 5, (2014) January, pp. 1229-1236.
- [8] W. Gu, Z. Lv and M. Hao, "Change detection method for remote sensing images based on an improved Markov random field", *Multimedia Tools and Applications*, (2015), pp. 1-16.
- [9] Z. Chen, W. Huang and Z. Lv, "Towards a face recognition method based on uncorrelated discriminant sparse preserving projection", *Multimedia Tools and Applications*, (2015), pp. 1-15.
- [10] J. Hu and Z. Gao, "Distinction immune genes of hepatitis-induced hepatocellular carcinoma", *Bioinformatics*, vol. 28, no. 24, (2012), pp. 3191-3194.
- [11] T. Su, W. Wang and Z. Lv, "Rapid Delaunay triangulation for randomly distributed point cloud data using adaptive Hilbert curve", *Computers & Graphics*, vol. 54, (2016), pp. 65-74.
- [12] W. Gu, Z. Lv and M. Hao, "Change detection method for remote sensing images based on an improved Markov random field", *Multimedia Tools and Applications*, (2015), pp. 1-16.
- [13] Z. Lv, A. Tek and F. Da Silva, "Game on, science-how video game technology may help biologists tackle visualization challenges", *PloS one*, vol. 8, no. 3, (2013), pp. 57990.

Author



LI Jun, received his B.S. degree in Electrical engineering from HUAZHONG University of science and technology in wuhan, China. He research interest is mainly in the area of power electronics technology and Computer Software. He has published several research papers in scholarly journals in the above research areas and has participated in several books.